



Calibrating soybean parameters in JULES 5.0 from the US-Ne2/3 FLUXNET sites and the SoyFACE-O₃ experiment

Felix Leung^{1,3}, Karina Williams^{2,7}, Stephen Sitch¹, Amos P.K. Tai^{3,6}, Andy Wiltshire², Jemma Gornall², Elizabeth A. Ainsworth⁴, Timothy Arkebauer⁵, David Scoby⁵

5 ¹ College of Life and Environmental Sciences, University of Exeter, Exeter, EX4 4RJ, UK.

²Met Office Hadley Centre, FitzRoy Road, Exeter, Devon, United Kingdom

³Earth System Science Programme, Faculty of Science, and Institute of Environment, Energy and Sustainability, The Chinese University of Hong Kong, Hong Kong

⁴USDA ARS, Global Change and Photosynthesis Research Unit, Urbana, Illinois, USA

10 ⁵ Department of Agronomy and Horticulture, University of Nebraska-Lincoln, Lincoln, Nebraska, USA

⁶ State Key Laboratory of Agrobiotechnology, The Chinese University of Hong Kong, Hong Kong

⁷Global System Institute, University of Exeter, Laver Building, North Park Road, Exeter EX4 4QE, UK

Correspondence to: Felix Leung (felix.leung@cuhk.edu.hk)

Abstract. Tropospheric ozone (O₃) is the third most important anthropogenic greenhouse gas. O₃ is detrimental
15 to plant productivity, and it has a significant impact on crop yield. Currently, the Joint UK Land Environment
Simulator (JULES) land surface model includes a representation of global crops (JULES-crop), but does not have
crop-specific O₃ damage parameters, and applies default C3 grass O₃ parameters for soybean that underestimates
O₃ damage. Physiological parameters for O₃ damage in soybean in JULES-crop were calibrated against leaf gas-
exchange measurements from the Soybean Free-Air-Concentration-Enrichment (SoyFACE) with O₃ experiment
20 in Illinois, USA. Other plant parameters were calibrated using an extensive array of soybean observations such
as crop height, leaf carbon, etc. and meteorological data from FLUXNET sites near Mead, Nebraska, USA. The
yield, aboveground carbon and leaf area index (LAI) of soybean from the SoyFACE experiment were used to
evaluate the newly calibrated parameters. The result shows good performance for yield, with the modelled yield
being within the spread of the SoyFACE observations. Although JULES-crop is able to reproduce observed LAI
25 seasonality, its magnitude is underestimated. The newly calibrated version of JULES will be applied regionally
and globally in future JULES simulations. This study helps to build a state-of-the-art impact assessment model
and contribute to a more complete understanding of the impacts of climate change on food production.



1 Introduction

30

Surface ozone (O₃) pollution is one of the major threats to global food security due to the detrimental effects of ozone exposure on crops (Ainsworth et al., 2012; Avnery et al., 2011b; Leung et al., 2020; Long et al., 2005; Tai et al., 2014; Tai and Val Martin, 2017). In the United States alone, crop loss due to tropospheric O₃ costs more than \$5 billion USD annually (Ainsworth et al., 2012; Avnery et al., 2011a; Van Dingenen et al., 2009).

35

Soybean is one of the main staple crops for human consumption; it also serves as an important source of animal feed. It is a cheap source of proteins and therefore soybean products are consumed around the world. The impact of O₃ on soybean physiology and growth has been studied extensively (Ainsworth et al., 2012; Betzelberger et al., 2012; Dermody et al., 2008; Morgan et al., 2003). Crop yield losses to tropospheric O₃ have been quantified using
40 model projection and experiments. The National Crop Loss Assessment Network and European Open Top Chamber programs have established the air quality guideline, which derived dose-response relationships from comparable experimental data. These campaigns provided critical information such as the O₃ response relationship and estimated yield loss due to O₃ damage that enabled regional projections of O₃ effects on crop yields (Fuhrer, 2009). However, open top chambers modify plant response to O₃ due to the ‘chamber effects’ which create
45 microclimates (Elagöz and Manning, 2005) and environmental differences between the chamber and open air micrometeorology in which yield loss is underestimated (Van Dingenen et al., 2009). Recently the introduction of Free-Air-Concentration-Enrichment (FACE) technology avoids the artefacts from enclosed chambers, and O₃ fumigation was adapted to FACE facilities (Morgan et al., 2004). The application of FACE experiment on crops took place in China (Zhu et al., 2011) and USA, including experiments with soybean at the
50 SoyFACE experiment in Champaign, Illinois (Morgan et al., 2004; Betzelberger et al. 2010; 2012).

55

Crops are a significant component of the land surface; e.g., croplands and pasturelands represent 12% and 26% of the global terrestrial land, respectively (Van den Hoof et al., 2011). Moreover, the phenology of crops is very different from that of natural vegetation, and is characterized by high growth, turnover rate, and strong seasonality. It is thus necessary to include a crop-specific parameterization scheme to improve simulations of land surface fluxes and regional climate in agroecosystems (Van den Hoof et al., 2011). The Joint UK Land Environment Simulator with crops (JULES-crop) is a crop parameterisation (Osborne et al., 2015) within the land surface model, JULES (Best et al., 2011; Clark et al., 2011). Global simulations have been performed with JULES-crop for rice, wheat, maize and soybean (Osborne et al., 2015). These four crop types contribute more



60 than 70% of human calorie intake (Ray et al., 2013). JULES-crop includes routines representing growth,
development and harvesting of crops driven by the overlying meteorological inputs. In JULES-crop, four new
prognostic variables have been added: crop development index (DVI), root carbon (Croot), harvest carbon
(Charv) and reserve carbon (Cresv). DVI controls the duration of the crop growing season in four distinct stages:
sowing, emergence, flowering, and maturity, and it determines when changes in carbon partitioning occur
65 (Osborne and Hooker, 2011). Croot, Charv, and Cresv are the carbon pools for roots, harvested organs (e.g.
grains of cereal, fruits, and root) and stem reserves, respectively. Carbon pools for stem and leaves are determined
from the existing prognostic variables, LAI (Leaf area index) and canopy height. In Osborne et al. (2015), global
runs of maize, wheat, soybean and rice were carried out using JULES-crop. Site runs were performed at four
70 FLUXNET sites with soybean-maize rotation: Bondville (US-Bo1), Fermi (US-IB1) and Mead (US-Ne2 and
US-Ne3). Simulated yield was compared against country and global FAO crop yields. Osborne et al. (2015)
used generic representations for each of the crops in their global study. For the plant parameters that are needed
outside the crop model such as leaf nitrogen and leaf respiration parameters, these are set to those of the C3 or
C4 grass functional types. Osborne et al. (2015) suggested that these parameters could be tuned to be more crop
specific to improve fit to observations. These JULES parameters have been calibrated against observations for
75 maize, using data from the Mead FLUXNET sites in Nebraska (Williams et al., 2017). However, to date, these
parameters have not been calibrated to soybean data.

There are many crop models developed by institutions / organisations around the world. Most are designed for
application to an individual field up to the regional scale and do not include O₃ impacts on vegetation.
80 (Appendix Table A1) compares a selection of land surface models which include crop tiles and have the
functions to model climate impact on crop productivity. JULES-crop is of particular interest because it is a
development of the global land surface component JULES of the Met Office numerical weather prediction and
climate models, and contains a detailed representation of plant physiological processes at sub-diurnal
timescales, including consideration of O₃ effects on natural vegetation, thus making it suitable for this study.
85 JULES-Crop has been accepted into the JULES trunk with the intention to be coupled with the Hadley Centre
Global Environment Model (HadGEM) in the near future. HadGEM is recognised as one of the best
performing climate models with smaller errors than typical climate models (Gleckler et al., 2008; Knutti et al.,
2013).

90



The calibration of O₃ damage on soybean would allow land surface and crop models to more realistically and reliably simulate present-day and future O₃ damage, and subsequently to quantify its economic impacts. The objective of this study is to calibrate soybean representation for JULES-crop, with a particular focus on the response of soybean to O₃ exposure.

95

This paper is organised as follows: Section 2 describes the model set-up and observations used for the JULES calibration. Section 3 compares the results from the calibrated JULES runs against independent observations. Section 4 assesses the suitability of the model for modelling soybean under O₃ damage and discusses ways of future model improvement.

100

2 Methods

A flowchart demonstrating the calibration and evaluation procedure is given in Figure 1. We first tuned the JULES-crop soybean parameterisation at the US-Ne2 and US-Ne3 Mead sites, where ten years of soybean physiological and meteorological observations were available, at ambient ozone (Figure 1, steps 1-5).

105

Secondly, to calibrate the JULES ozone damage parameters (Figure 1, step 6) we made the assumption that there is a negligible damage to crop yield at ambient background levels of O₃ at both the SoyFACE and Mead sites. This is consistent with Mills et al. (2007), who reviewed over 700 published papers and conference proceedings and found that O₃ level of AOT40 over 3 months of 5 ppm-h reduced soybean yield by less than 5%. Then we calibrated specifically the soybean O₃ response using leaf gas exchange measurements from soybean grown under elevated O₃ concentrations at SoyFACE.

110

Finally, we applied JULES-crop newly calibrated for soybean and its O₃ sensitivity at the leaf-level and evaluated model performance against observed yield and leaf area index from SoyFACE, taken for the full range of rings and cultivars (Figure 1, step 7).

115

2.1 Calibration of soybean in the absence of ozone damage, using observations from Mead

We followed the standard tuning procedure performed on maize by Williams et al., (2017) but applied to soybean (Figure 1, steps 1-5). This method is described in detail in the Supplementary Material, and the resulting

120



parameters are given in Table 1-3. These are compared to the parameters used in Osborne et al. (2015), which we refer to as the “Osborne 2015 tuning”. Note that the parameters in Table 3 in the Osborne 2015 tuning are typical defaults for C3 grass, rather than soybean-specific.

125

2.2 Calibration of JULES ozone damage parameters

2.2.1 Ozone effects on vegetation (exposure-response)

Many studies have shown that the impacts of O₃ are closely related to accumulated exposure above a threshold concentration rather than the mean growing season concentration (Forestry Commission, 2016; Gerosa et al. 2012; Mills et al. 2007). An index of accumulated exposure above a threshold concentration of x ppb (AOT_x) has thus been developed as a measure of assessing O₃ pollution effects on vegetation. AOT_x is calculated as the summed product of the concentration above the threshold concentration and time (T), with values expressed in ppb h or ppm h. (Mills et al. 2007; Forestry Commission, 2016).

135 The O₃ exposure index AOT₄₀: Accumulated O₃ exposure over a threshold of 40 parts per billion (Equation 1) has been widely used by crop impact models in the forestry and agriculture industry and was used at SoyFACE.

$$AOT_{40} = \int \max(O_3 - 40ppb, 0.0) dt \quad (1)$$

The metric ensures only O₃ concentrations above 40 ppb are included. The integral is taken over daytime hours. AOT₄₀ does not account for the actual uptake of O₃ by plants and how this varies with ontogenetic (life span of the plant) and climatic factors such as temperature, irradiance, vapour pressure deficit, and/or soil moisture (Ashmore, 2005; Fuhrer et al. 1997).

There is a drawback of the cumulative O₃ exposure indices (Pleijel et al. 2000), which assume an instantaneously fixed threshold flux below which there is no effect of O₃, which may not be realistic. Also in nature, the threshold value is unlikely to be constant (Ashmore, 2005) since the capacity of detoxification of O₃ varies with climate and plant species. To improve these indices, the Stockholm Environment Institute developed the Deposition of Ozone for Stomatal Exchange model (DO₃SE) (Emberson et al., 2007). DO₃SE was developed to estimate the risk of O₃ damage to European vegetation and is capable of providing O₃ flux estimation by evaluating the soil water deficits and their influence on stomatal conductance which affect plant O₃ uptake. Phyto-toxic O₃ dose (POD) above a stomatal threshold over a growing season (the accumulated stomatal flux above threshold Y) POD_y can differentiate species sensitivity to rising background concentration, while AOT₄₀ can only incorporate the effect

150



of rising global background O₃ above the threshold 40ppb. This difference means AOT40 metric is less sensitive to O₃ peaks, and stomatal flux based metric (e.g. PODy and DO3SE) perform better on O₃ damage estimation in general (Büker et al., 2012; Dentener, F., Keating, T., and Akimoto, 2010; Pleijel et al., 2007).

155

2.2.2 Description of ozone response scheme in JULES

The current O₃ scheme in JULES uses a dose-response approach to model O₃ damage (Sitch et al., 2007; Clark et al., 2011). It uses the O₃ concentration in the atmosphere to modify net photosynthesis A_p by an O₃ uptake factor f :

160

$$A = A_p f \quad (2)$$

where f represents the fractional reduction of plant production:

$$f = 1 - a U_{O_3 > FO_{3crit}} \quad (3)$$

165 It assumes that O₃ suppresses the potential net leaf photosynthesis in proportion to the O₃ flux through stomata above a specified critical threshold (Clark et al., 2011).

$U_{O_3 > FO_{3crit}}$ is the instantaneous leaf uptake of O₃ over a plant functional type specific threshold (FO_{3crit}) (nmol m⁻²s⁻¹) and the plant type specific parameter a is the fractional reduction of photosynthesis with O₃ uptake by leaves (Clark et al., 2011; Sitch et al., 2007).

170

$$U_{O_3 > FO_{3crit}} = \max[(F_{O_3} - FO_{3crit}), 0.0] \quad (4)$$

From equations 3 & 4, F depends on the O₃ uptake rate by stomata (F_{O_3}) over a critical (plant functional type specific) threshold for damage. It uses an analogy of Ohm's law, the O₃ flux through stomata, F_{O_3} (nmol O₃ m⁻² s⁻¹), is given by,

175

$$F_{O_3} = \frac{[O_3]}{R_a + \left[\frac{K_{O_3}}{g_l} \right]} \quad (5)$$



180 where $[O_3]$ is the molar concentration of O_3 at reference level ($nmol\ m^{-3}$), R_a is the combined aerodynamic and boundary layer resistance between leaf surface and reference level ($s\ m^{-1}$). g_l is the leaf conductance for H_2O ($m\ s^{-1}$), and $\kappa_{O_3} = 1.67$ is the ratio of leaf resistance for O_3 to leaf resistance for water vapour [Sitch et al., 2007]. The uptake flux is dependent on the stomatal conductance, which is reliant on the photosynthetic rate in JULES. Given that g_l and photosynthetic rate A are linear related [Cox et al., 1999], g_l is given by,

$$g_l = g_p f \quad (6)$$

185

Where g_p is the leaf conductance in the absence of O_3 effects. The set of equations (3,5,6) produces a quadratic relationship as a function of f , that can be solved analytically (Sitch et al., 2007).

190 Fractional reduction of photosynthesis with the instantaneous uptake of O_3 by leaves ($mmol\ m^{-2}$) (dfp_dcuo_io) determines the sensitivity of soybean to O_3 and the PFT-specific O_3 critical level ($FO_3\ crit$) determines the threshold O_3 flux which would cause damage to photosynthesis (Oliver et al., 2018; Sitch et al., 2007). The higher the sensitivity of plants to O_3 the lower photosynthesis the plant has at a given constant critical threshold. Sitch et al. (2007) configured plant functional types with two different O_3 sensitivities (fractional reduction of photosynthesis by O_3 , F , equation 1, 2), where $F = 1.40$ is high sensitivity, and $F = 0.25$ is lower sensitivity for
195 C3 grass (Sitch, 2007), using monthly average O_3 data and calibration to yield observations.

2.2.4 Calibrating the ozone effects on crop leaf photosynthesis in JULES using SoyFACE

200 The SoyFACE experiment in Illinois allows controlled CO_2 or O_3 enrichment across large plots within a soybean field without an enclosure. SoyFACE O_3 fumigation typically began after the emergence of soybean, and the plots were fumigated with O_3 for 8–9 hours daily except when leaves were wet. In 2009 and 2010, soybeans were exposed to nine different concentrations of O_3 ranging from the ambient level to a target level of 200 ppb (Figure A2). The fumigation ended when soybean was mature.

205 Plant damage from O_3 is cumulative and the target concentration for the experiment was not always met (e.g., when wind speeds are low, during rain or when O_3 generators or analyzers are down). Therefore, the 8-hour mean and the AOT40 index (Accumulated Ozone exposure above the Threshold of 40 ppb) were used for the analysis in SoyFACE instead of using the target O_3 concentration. The planting dates were June 6, 2009 (Day 159) and May 27, 2010 (Day 157). Fumigation began on June 29, 2009 (Day 179 - 260) and June 6, 2010 (Day 167 - 271) and harvest occurred on October 20, 2009 (Day 293) and September 20, 2010 (Day 273). O_3 concentrations



210 measured at SoyFACE fluctuated greatly, as they were strongly influenced by weather conditions, especially by
wind speed. The magnitude of O₃ concentration fluctuations in the high targeted concentration was greater than
the low concentration (Figure A2). On some days of the year when the fumigation was off, very low O₃
concentrations were recorded for all target rings.

215 To calibrate the O₃ parameters for soybean in JULES-crop, we used midday photosynthetic gas-exchange
measurements from Betzelberger et al. (2012). These were taken at four stages during the growing season, from
seven soybean cultivars growing at 9 different O₃ concentrations, using open gas exchange systems (LI-6400 and
LI-6400-40). These observations were used in conjunction with the daytime 8-hour mean O₃ concentration
220 measurements and the parameters calibrated at the Mead site to drive the Leaf Simulator computer package, which
reproduces the calculation of leaf photosynthesis within JULES. We then tuned the O₃ parameterisation of
Fractional reduction of photosynthesis by O₃ (sensitivity) and Threshold of O₃ flux (mmol m⁻² s⁻¹) to match the
modelled leaf photosynthesis rate to the observed rate (Figure 2). The tuned parameters are showed in Table 4.

225

2.3 Model configuration for the JULES-crop SoyFACE runs

The meteorological forcing data measured at Champaign, Illinois in 2009 (Ainsworth et al., 2010) were used to
drive the JULES-crop model. The downward longwave radiation and diffuse radiation data from NOAA at
230 Bondville site (SURFRAD) were used as SoyFACE does not have these variables available. The driving data were
repeatedly applied (recycled 25 times) to spin up the model from an arbitrary starting point with soil temperature
initially set to 278 K and soil moisture to 75% of saturation. A single crop type was modelled – soybean – using
a single plant tile. Observed CO₂ (NOAA) and 8-hour mean observed O₃ concentrations from the SoyFACE rings
(averaged over a month) were used as the driving data of the model since natural O₃ is produced around 8 hours
235 in daytime and it is a typical temporal resolution for O₃ fumigation. The soil ancillary parameters used in
SoyFACE were extracted from the global dataset of soil ancillary from the HadGEM2-ES model (a coupled Earth
System Model that was used by the Met Office Hadley Centre for the CMIP5). Observed ambient O₃ were used
as the control. The new parameters for soybean were used, which we calibrated to observations from the Mead
FLUXNET sites as described in the supplementary material. The exception is the initial carbon: since the row
240 spacing at the SoyFACE experiment is half that used at the Mead sites, we doubled the initial carbon for SoyFACE



compared to Mead. The resulting model yield, above ground carbon and LAI was compared to the SoyFACE observations.

245 3 Results and Discussion

3.1 Results from JULES runs with crop model and ozone damage turned on

Figure 3 shows the evaluation of the soybean aboveground biomass carbon for different O₃ exposure levels (AOT40) using the O₃ damage parameters in Table 4. The model aboveground carbon (solid lines) are compared to the line fitted in Betzelberger et al 2012 to their aboveground carbon observations. The run with the newly-calibrated parameters overestimated the carbon at ambient ozone levels. One contributing factor could be that water stress is underestimated in the new configuration, since it was not possible to evaluate the response to soil water availability using the Mead site data, so we instead derived a value for p₀ (parameterise in the calculation of the threshold for water stress, see Table 3) from literature. We tested the sensitivity to this choice by re-running this configuration with p₀=0, and this caused a 12% reduction in aboveground carbon (plots not shown). In addition, the representation of the soil properties in the JULES SoyFACE run could be improved by calibration to site measurements. In contrast, the “Osborne 2015 tuning” intersects the line fitted to observed aboveground carbon at zero ozone concentration (partially because of higher water stress), but then shows a sharp decrease from zero to ambient levels, which is not realistic. Note that no observations were taken for below-ambient ozone concentrations at SoyFACE, so this section of the fitted line is an extrapolation. The slope of the aboveground carbon response to increasing ozone concentrations is similar for all three runs, and compares very well to the Betzelberger et al 2012 fitted line.

The yield-O₃ response curve in Figure 4 show that new parametrisation slightly overestimates yield in the ambient SoyFACE ring, compared to the spread of SoyFACE yield observations from Betzelberger et al 2012. The ‘Osborne 2015 tuning’ with high ozone sensitivity is within the spread of measured yield in ambient conditions, but note that the modelled yield has decreased sharply from zero ozone concentration to ambient levels, which is undesirable. The magnitude of the gradient of yield against AOT40 for all three model configurations is within the spread of the observations. However, the slope is underestimated for the new, calibrated run and overestimated for the ‘Osborne 2015 tuning’, especially for the range from ambient to 40 ppm h. Recall that ozone concentration modifies net leaf CO₂ assimilation rate in JULES, and that the model parameters governing this process (*Fo3crit*,



275 *a*) are calibrated directly to net leaf CO₂ assimilation rate observations from SoyFACE in our new configuration (Section 2). Reductions in the modelled net leaf CO₂ assimilation rate lead to the reductions in model aboveground biomass, yield and LAI which we show in this section. However, Betzelberger et al 2012 also reported additional impacts of ozone damage, such as changes in leaf absorptance and specific leaf mass, that are not represented in JULES, and therefore our tuning does not account for them. In contrast, the values of *Fo3crit* and *a* in the high and low sensitivity versions of the ‘Osborne 2015 tuning’ simulations (table 4) were calibrated in Sitch et al 2007 to yield observations. Therefore, they can be seen as ‘effective’ parameters in these configurations, since they incorporate the effect of the ozone damage processes that are not explicitly represented in JULES.

280

Note that we plot AOT40 on the x-axis for illustrative purposes only, to be comparable with results presented in Betzelberger et al 2012 - AOT40 was not used in the JULES run. An alternative would be to plot ring number or ring target concentration. Ideally, we would plot the x-axis with the metric Phytotoxic Ozone Dose (POD) for JULES and observed data, which account the dosage of O₃ that get into the stomata of soybean, but is beyond the scope of the present study.

290 Figure 5 compares the model and observed LAI at SoyFACE for different O₃ concentrations. JULES was able to reproduce LAI seasonality; however, it underestimated the amplitude. The maximum LAI for calibrated JULES peaked around day 240 in September and observations peaked at DOY 220~230. The peak LAI in the model runs was less than half the observed LAI in all cases. While the Mead model runs also showed a slight underestimation of peak LAI compared to observation (Supplementary Materials), the majority of the underestimation of the modelled SoyFACE LAI is due to a difference between the observed relationships between peak LAI and yield at the Mead and SoyFACE sites. At both sites, observed maximum yield increases with observed peak LAI. However, for similar observed yields, the observed SoyFACE yield tends to be higher than the observed Mead LAI. Given that our calibration is based on Mead observations, it is therefore not surprising that our model runs at SoyFACE underestimate peak LAI compared to the SoyFACE observations.

300 A contributing factor to the different relationship between observed peak LAI and observed yield at SoyFACE compared to Mead could be the different methods used to measure LAI at the Mead sites (which this parameter set was tuned against) and at SoyFACE. At Mead, destructive measurements were taken, whereas at SoyFACE, LAI was measured indirectly, using radiation attenuation through the canopy.



Another plausible contributing factor for the different relationship between observed peak LAI and observed yield
305 at SoyFACE compared to Mead is the row density of the soybean. The SoyFACE row spacing was half that of
Mead so, as described above, we set the initial carbon to twice that observed at Mead. The denser planting allowed
soybean at SoyFACE to reach higher LAI earlier in the growing season. If this also resulted in thinner leaves at
the beginning of the season than with the Mead row spacing, then this could explain the difference in the peak
LAI to yield relationship between the two sites. JULES also does not account for leaf age on leaf assimilation rate
310 - in reality a lower leaf assimilation is observed in the late season associated with leaf aging, and it is plausible
that this could also be affected by row spacing.

Figure 5 also demonstrates that model LAI responds more to ozone concentrations than the observed LAI. One
contributing factor is the observed decrease in specific leaf area at SoyFACE in increased ozone (Betzberger et
315 al 2012). As mentioned above, this process is not captured by JULES. This issue is particularly pronounced in the
Osborne 2015 tuning runs, where the modelled LAI in the ring with target 200ppb is roughly a third of the peak
LAI in the ambient ring.

320 **5 Conclusions**

Climate change and air pollution are a great threat to food production. JULES-crop has been developed to
represent crops in the land surface model and allow us to estimate the future climate and air pollution impact to
crops. The O₃ impact on crops could be quantified with an improved parameterization to the existing O₃ damage
scheme for C3 plants. The default soybean biochemical and respiratory parameters in JULES were based on C3
325 grass parameters. Characteristics of soybean are more similar to a shrub than grass, therefore parameter calibration
is needed to improve the performance of soybean in JULES-crop.

In this paper, the parameters needed to describe soybean in JULES-crop were first revised against observations
from the Mead FLUXNET sites to ensure that the crop, biochemical and respiratory parameters explicitly
330 represented soybean. Compared with observations from these sites showed that GPP and LAI were well
represented for irrigated soybean at Mead. The O₃ damage parameterisation was subsequently calibrated against
leaf gas exchange observations from the Soybean Free-Air-Concentration-Enrichment (FACE) experiment for the
O₃ damage, by tuning the sensitivity and critical threshold of O₃ damage. On the whole, JULES-Crop reproduces



335 the observed negative correlation between yield and O₃ exposure. It also reproduced the negative impacts of ozone
on LAI, and the seasonality of phenology, although the simulated LAI was underestimated at SoyFACE. This
method of calibrating soybean could be replicated for other crops once data become available and would contribute
to more accurate parameters for crop models. The calibration will be applied to a regional and transient run and
eventually the newly calibrated JULES-crop for soybean and its sensitivity to O₃ damage, coupled within an Earth
System Model.

340

Code availability. This study uses JULES version 5.0 releases. The code and configuration for the SoyFACE
runs can be downloaded via the Met Office Science Repository Service (MOSRS) at
<https://code.metoffice.gov.uk/trac/roses-u/browser/a/r/8/6/6/trunk> (JULES Collaboration, 2018)(registration
345 required) and are freely available subject to completion of a software licence. The Leaf Simulator can be
downloaded from <https://code.metoffice.gov.uk/trac/utills> (Williams et al., 2018) (login required).

350 *Data availability.* Unless otherwise noted, all site observations discussed in this paper were obtained from the
Site Information pages of the AmeriFlux website hosted by Oak Ridge National Laboratory
(<http://fluxnet.fluxdata.org/>, (AmeriFlux collaboration, 2018)) or by personal communication with the Mead sites
Research Technologist. The longwave radiation, diffuse radiation and air pressure from Bondville, Illinois site is
obtained by the SURFRAD (Surface radiation) network from
355 ftp://aftp.cmdl.noaa.gov/data/radiation/surfrad/Bondville_IL/. The SoyFACE data used for the run are available
on MOSRS at:

https://code.metoffice.gov.uk/trac/roses-u/browser/a/r/8/6/6/trunk/driving_data

https://code.metoffice.gov.uk/trac/roses-u/browser/a/r/8/6/6/trunk/bin/SoyFACE_gas_exchange_data_2009.csv

https://code.metoffice.gov.uk/trac/roses-u/browser/a/r/8/6/6/trunk/ancil_data

360 Accessing the MOSRS requires registration, but once you access into the system, there's no information about
who is downloading or viewing which pages.

Acknowledgements. Felix Leung gratefully acknowledges financial support from the NERC CASE Studentship
with Met Office (NE/J017337/1), “Impact of tropospheric O₃ on crop production under future climate and



365 atmospheric CO₂ concentrations, and their interactions within the Earth System”. Karina Williams gratefully acknowledges financial support from the European Commission under grant agreements 308291 (EUPORIAS), 603864 (HELIX). We acknowledge the following AmeriFlux sites for their data records: US-Ne1, US-Ne1, US-Ne3. In addition, funding for AmeriFlux data resources and core site data was provided by the U.S. Department of Energy’s Office of Science.



370 **References**

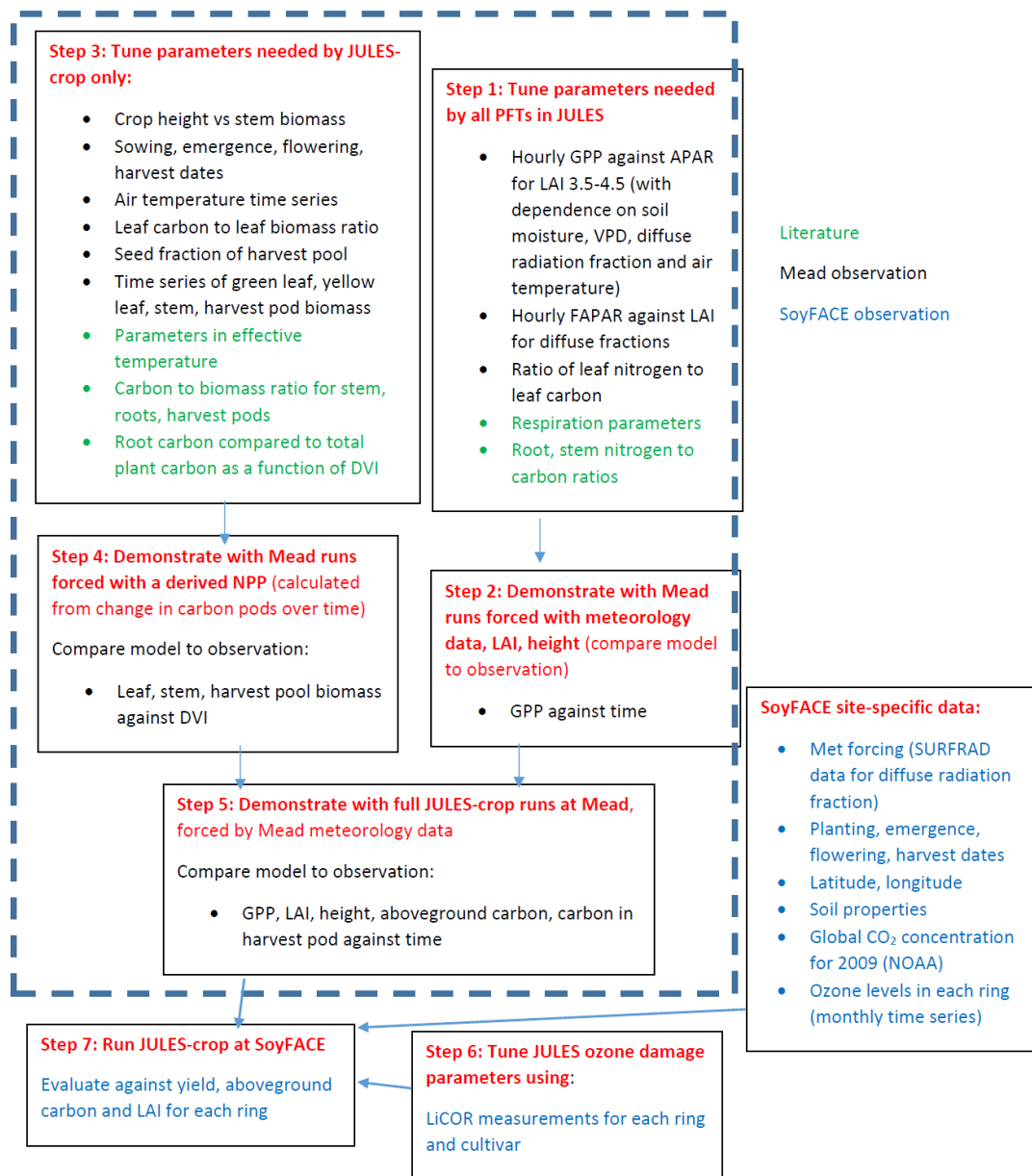
- Ainsworth, E. a, Yendrek, C. R., Sitch, S., Collins, W. J. and Emberson, L. D.: The effects of tropospheric ozone on net primary productivity and implications for climate change., *Annu. Rev. Plant Biol.*, 63, 637–61, doi:10.1146/annurev-arplant-042110-103829, 2012.
- Allen, R. G. and Pereira, L. S.: Crop Evapotranspiration (guidelines for computing crop water requirements), Rome. [online] Available from: <https://www.kimberly.uidaho.edu/water/fao56/fao56.pdf> (Accessed 28 September 2018), 2006.
- AmeriFlux collaboration: AmeriFlux Site Information, [online] Available from: <http://fluxnet.fluxdata.org/> (Accessed 11 November 2018), 2018.
- Ashmore, M. R.: Assessing the future global impacts of ozone on vegetation, *Plant, Cell Environ.*, 28(8), 949–964, doi:10.1111/j.1365-3040.2005.01341.x, 2005.
- 380 Avnery, S., Mauzerall, D. L., Liu, J. and Horowitz, L. W.: Global crop yield reductions due to surface ozone exposure: 1. Year 2000 crop production losses and economic damage, *Atmos. Environ.*, 45(13), 2284–2296, doi:10.1016/j.atmosenv.2010.11.045, 2011a.
- Avnery, S., Mauzerall, D. L., Liu, J. and Horowitz, L. W.: Global crop yield reductions due to surface ozone exposure: 2. Year 2030 potential crop production losses and economic damage under two scenarios of O₃ pollution, *Atmos. Environ.*, 45(13), 2297–2309, doi:10.1016/j.atmosenv.2011.01.002, 2011b.
- 385 Best, M. J., Pryor, M., Clark, D. B., Rooney, G. G., Essery, R. . L. H., Ménard, C. B., Edwards, J. M., Hendry, M. A., Porson, A., Gedney, N., Mercado, L. M., Sitch, S., Blyth, E., Boucher, O., Cox, P. M., Grimmond, C. S. B. and Harding, R. J.: The Joint UK Land Environment Simulator (JULES), model description – Part 1: Energy and water fluxes, *Geosci. Model Dev.*, 4(3), 677–699, doi:10.5194/gmd-4-677-2011, 2011.
- 390 Betzelberger, A. M., Yendrek, C. R., Sun, J., Leisner, C. P., Nelson, R. L., Ort, D. R. and Ainsworth, E. a: Ozone exposure response for U.S. soybean cultivars: linear reductions in photosynthetic potential, biomass, and yield., *Plant Physiol.*, 160(4), 1827–39, doi:10.1104/pp.112.205591, 2012.
- Büker, P., Morrissey, T., Briolat, a., Falk, R., Simpson, D., Tuovinen, J.-P., Alonso, R., Barth, S., Baumgarten, M., Grulke, N., Karlsson, P. E., King, J., Lagergren, F., Matyssek, R., Nunn, a., Ogaya, R., Peñuelas, J., Rhea, L., Schaub, M., Uddling, J., Werner, W. and Emberson, L. D.: DO₃SE modelling of soil moisture to determine ozone flux to forest trees, *Atmos. Chem. Phys.*, 12(12), 5537–5562, doi:10.5194/acp-12-5537-2012, 2012.
- 395 Clark, D. B., Mercado, L. M., Sitch, S., Jones, C. D., Gedney, N., Best, M. J., Pryor, M., Rooney, G. G., Essery, R. L. H., Blyth, E., Boucher, O., Harding, R. J., Huntingford, C. and Cox, P. M.: The Joint UK Land Environment Simulator (JULES), model description – Part 2: Carbon fluxes and vegetation dynamics, *Geosci. Model Dev.*, 4(3), 701–722, doi:10.5194/gmd-4-701-2011, 2011.
- Dentener, F., Keating, T., and Akimoto, H.: Hemispheric Transport of 2010 Part a : Ozone and Particulate Matter, *Air Pollution Study*, (17), 278. [online] Available from: https://www.unece.org/fileadmin/DAM/env/lrtap/Publications/11-22136-Part-D_01.pdf
- 405 Dermody, O., Long, S. P., McCONNAUGHAY, K. and DeLUCIA, E. H.: How do elevated CO₂ and O₃ affect the interception and utilization of radiation by a soybean canopy?, *Glob. Chang. Biol.*, 14(3), 556–564, doi:10.1111/j.1365-2486.2007.01502.x, 2008.
- Van Dingenen, R., Dentener, F. J., Raes, F., Krol, M. C., Emberson, L. and Cofala, J.: The global impact of ozone on agricultural crop yields under current and future air quality legislation, *Atmos. Environ.*, 43(3), 604–618, doi:10.1016/j.atmosenv.2008.10.033, 2009.
- 410



- Elagöz, V. and Manning, W. J.: Responses of sensitive and tolerant bush beans (*Phaseolus vulgaris* L.) to ozone in open-top chambers are influenced by phenotypic differences, morphological characteristics, and the chamber environment, *Environ. Pollut.*, 136(3), 371–383, doi:10.1016/j.envpol.2005.01.021, 2005.
- Emberson, L. D., Büker, P. and Ashmore, M. R.: Assessing the risk caused by ground level ozone to European forest trees: A case study in pine, beech and oak across different climate regions, *Environ. Pollut.*, 147(3), 454–466, doi:10.1016/j.envpol.2006.10.026, 2007.
- 415 Fuhrer, J.: Ozone risk for crops and pastures in present and future climates., *Naturwissenschaften*, 96(2), 173–94, doi:10.1007/s00114-008-0468-7, 2009.
- Fuhrer, J., Skärby, L. and Ashmore, M. R.: Critical levels for ozone effects on vegetation in Europe., *Environ. Pollut.*, 97(1–2), 91–106 [online] Available from: <http://www.ncbi.nlm.nih.gov/pubmed/15093382>, 1997.
- 420 Gerosa, G., Finco, a., Marzuoli, R., Ferretti, M. and Gottardini, E.: Errors in ozone risk assessment using standard conditions for converting ozone concentrations obtained by passive samplers in mountain regions, *J. Environ. Monit.*, 14(6), 1703, doi:10.1039/c2em10965d, 2012.
- Gleckler, P. J., Taylor, K. E. and Doutriaux, C.: Performance metrics for climate models, *J. Geophys. Res.*, 425 113(D6), D06104, doi:10.1029/2007JD008972, 2008.
- Van den Hoof, C., Hanert, E. and Vidale, P. L.: Simulating dynamic crop growth with an adapted land surface model – JULES-SUCROS: Model development and validation, *Agric. For. Meteorol.*, 151(2), 137–153, doi:10.1016/j.agrformet.2010.09.011, 2011.
- JULES Collaboration: ULES collaboration: JULES land-surface model, [online] Available from: <https://code.metoffice.gov.uk/trac/jules/> (Accessed 11 November 2019), 2018.
- 430 Knutti, R., Masson, D. and Gettelman, A.: Climate model genealogy: Generation CMIP5 and how we got there, *Geophys. Res. Lett.*, 40(6), 1194–1199, doi:10.1002/grl.50256, 2013.
- Leung, F., Pang, J. Y. S., Tai, A. P. K., Lam, T., Tao, D. K. C. and Sharps, K.: Evidence of Ozone-Induced Visible Foliar Injury in Hong Kong Using *Phaseolus Vulgaris* as a Bioindicator, *Atmosphere (Basel)*, 11(3), 435 266, doi:10.3390/atmos11030266, 2020.
- Long, S. P., Ainsworth, E. a., Leahey, A. D. B. and Morgan, P. B.: Global food insecurity. treatment of major food crops with elevated carbon dioxide or ozone under large-scale fully open-air conditions suggests recent models may have overestimated future yields., *Philos. Trans. R. Soc. Lond. B. Biol. Sci.*, 360(1463), 2011–20, doi:10.1098/rstb.2005.1749, 2005.
- 440 Mills, G., Buse, A., Gimeno, B., Bermejo, V., Holland, M., Emberson, L. and Pleijel, H.: A synthesis of AOT40-based response functions and critical levels of ozone for agricultural and horticultural crops, *Atmos. Environ.*, 41(12), 2630–2643, doi:10.1016/j.atmosenv.2006.11.016, 2007.
- Morgan, P. B., Ainsworth, E. a. and Long, S. P.: How does elevated ozone impact soybean? A meta-analysis of photosynthesis, growth and yield, *Plant, Cell Environ.*, 26(8), 1317–1328, doi:10.1046/j.0016-8025.2003.01056.x, 2003.
- 445 Oliver, R. J., Mercado, L. M., Sitch, S., Simpson, D., Medlyn, B. E., Lin, Y.-S., Folberth, G. A. and Oliver, R. J.: Large but decreasing effect of ozone on the European carbon sink, *Biogeosciences*, 15, 4245–4269, doi:10.5194/bg-15-4245-2018, 2018.
- Osborne, T. and Hooker, J.: JULES-crop technical documentation Crop parameterisation, *Univ. Read.*, 1–49, 450 2011.

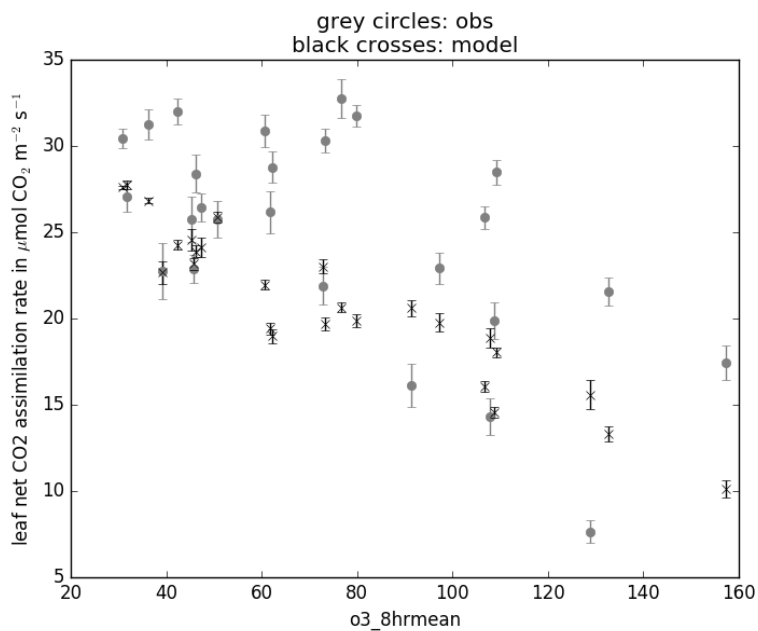


- Osborne, T., Gornall, J., Hooker, J., Williams, K., Wiltshire, A., Betts, R. and Wheeler, T.: JULES-crop: a
parametrisation of crops in the Joint UK Land Environment Simulator, *Geosci. Model Dev*, 8, 1139–1155,
doi:10.5194/gmd-8-1139-2015, 2015.
- Pleijel, H., Danielsson, H., Emberson, L., Ashmore, M. R. and Mills, G.: Ozone risk assessment for agricultural
455 crops in Europe: Further development of stomatal flux and flux–response relationships for European wheat and
potato, *Atmos. Environ.*, 41(14), 3022–3040, doi:10.1016/j.atmosenv.2006.12.002, 2007.
- Ray, D. K., Mueller, N. D., West, P. C., Foley, J. A., Pingali, P., Godfray, H., Beddington, J., Crute, I., Haddad,
L., Lawrence, D., Tilman, D., Balzer, C., Hill, J., Befort, B., Foley, J., Ramankutty, N., Brauman, K., Cassidy,
E., Gerber, J., Phalan, B., Balmford, A., Green, R., Scharlemann, J., Phalan, B., Onia, M., Balmford, A., Green,
460 R., Green, R., Cornell, S., Scharlemann, J., Balmford, A., Matson, P., Vitousek, P., Tscharntke, T., Clough, Y.,
Wanger, T., Jackson, L., Motzke, I., Hulme, M., Vickery, J., Green, R., Phalan, B., Chamberlain, D., Andrew,
D., Ephraim, C., Pingali, P., Cassman, K., Finger, R., Peltonen-Sainio, P., Jauhiainen, L., Laurila, I., Brisson,
N., Gate, P., Gouache, D., Charmet, G., Francois-Xavier, O., Lin, M., Huybers, P., Ray, D., Ramankutty, N.,
465 Mueller, N., West, P., Foley, J., Hafner, S., Dyson, T., Dawe, D., Dobermann, A., Moya, P., Abdurachman, S.,
Singh, B., Ladha, J., Dawe, D., Pathak, H., Padre, A., Yadav, R., Fischer, R., Edmeades, G., Jaggard, K., Qi, A.,
Ober, E., Supit, I., Foley, J., DeFries, R., Asner, G., Barford, C., Bonan, G., Rockström, J., Steffen, W., Noone,
K., Persson, A., Chapin, S., Donald, P., Green, R., Heath, M., Heathcote, A., Filstrup, C., Downing, J.,
Eickhout, B., Bouwman, A., et al.: Yield Trends Are Insufficient to Double Global Crop Production by 2050,
edited by J. P. Hart, *PLoS One*, 8(6), e66428, doi:10.1371/journal.pone.0066428, 2013.
- 470 Sitch, S.: Carbon sinks threatened by increasing ozone, *Nat. Publ. Gr.*, 7(8), 2335–40, doi:10.1021/nl0709975,
2007.
- Sitch, S., Cox, P. M., Collins, W. J. and Huntingford, C.: Indirect radiative forcing of climate change through
ozone effects on the land-carbon sink., *Nature*, 448(7155), 791–4, doi:10.1038/nature06059, 2007.
- Tai, A. P. K. and Val Martin, M.: Impacts of ozone air pollution and temperature extremes on crop yields:
475 Spatial variability, adaptation and implications for future food security, *Atmos. Environ.*, 169, 11–21,
doi:10.1016/J.ATMOSENV.2017.09.002, 2017.
- Tai, A. P. K., Martin, M. V. and Heald, C. L.: Threat to future global food security from climate change and
ozone air pollution, *Nat. Clim. Chang.*, 4(9), 817–821, doi:10.1038/NCLIMATE2317, 2014.
- Williams, K., Gornall, J., Harper, A., Wiltshire, A., Hemming, D., Quaife, T., Arkebauer, T. and Scoby, D.:
480 Evaluation of JULES-crop performance against site observations of irrigated maize from Mead, Nebraska,
Geosci. Model Dev, 10(3), 1291–1320, doi:10.5194/gmd-10-1291-2017, 2017.
- Williams, K., Hemming, D., Harper, A. B. and Mercado, L. M.: Leaf simulator, 2018.
- Zhang, J., Tian, H., Yang, J. and Pan, S.: Improving Representation of Crop Growth and Yield in the Dynamic
Land Ecosystem Model and Its Application to China, *J. Adv. Model. Earth Syst.*, 10(7), 1680–1707,
485 doi:10.1029/2017MS001253, 2018.



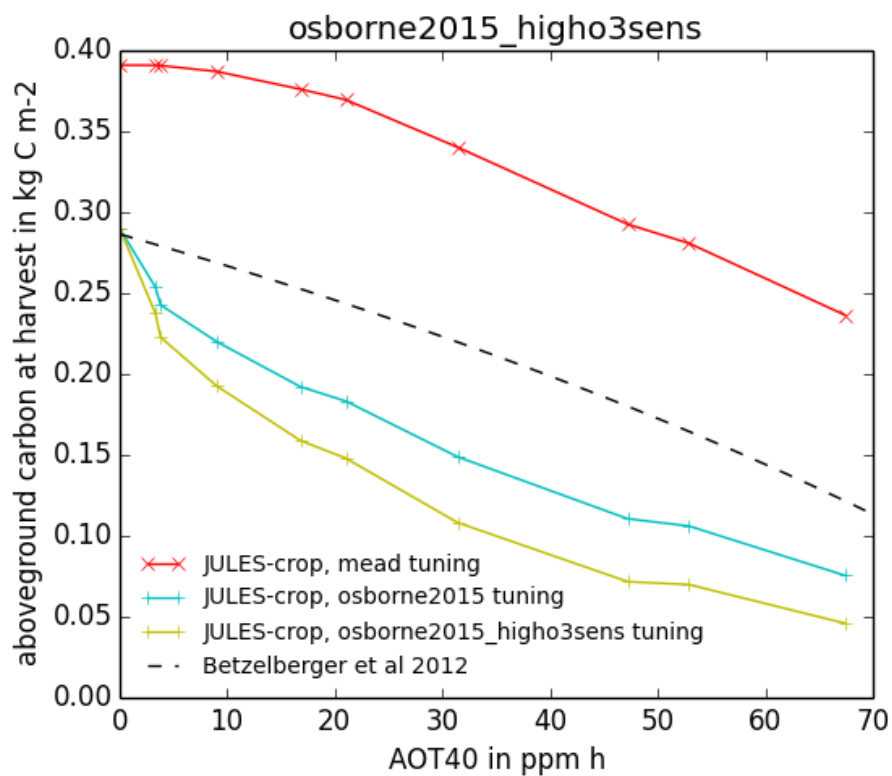
490

Figure 1. Flowchart of tuning the parameters and calibrating the model

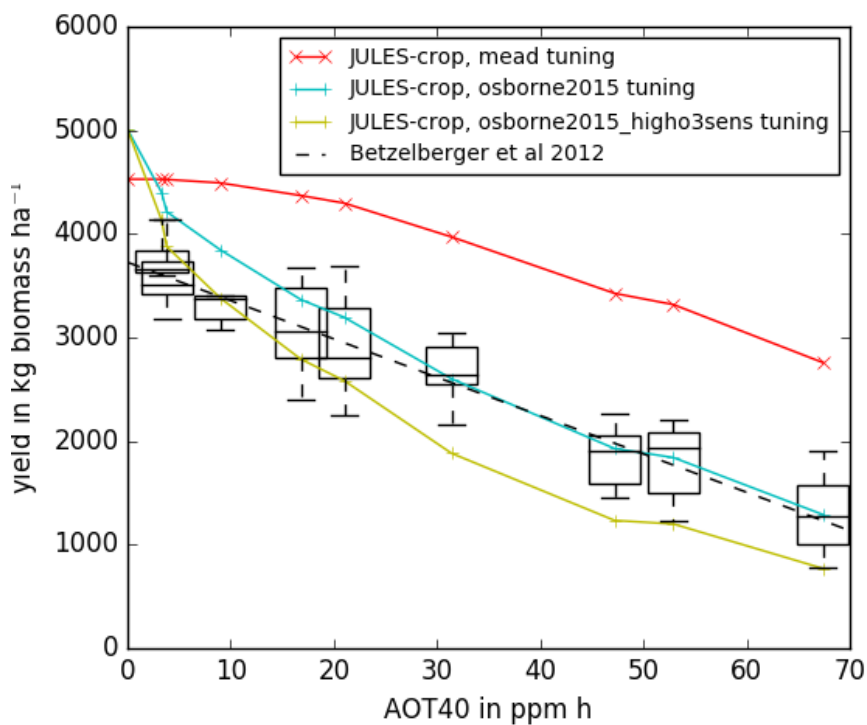


495

Figure 2. Net leaf CO₂ assimilation rate for calibrated JULES, simulated using the Leaf Simulator (black crosses) and observations from Betzelberger et al., (2012) (grey circles). X-axis is the daytime 8-hour mean O₃ concentration (ppb) .



500 **Figure 3.** Aboveground carbon biomass of soybean at harvest stage for calibrated Joint UK Land Environment Simulator with Crop module turned on (JULES-crop) using the Mead soybean tuning (red), Osborne et al. (2015) standard parameters with Sitch et al. (2007) low ozone sensitivity (blue), high ozone sensitivity (green) and observation from SoyFACE from Betzelberger et al. 2012.



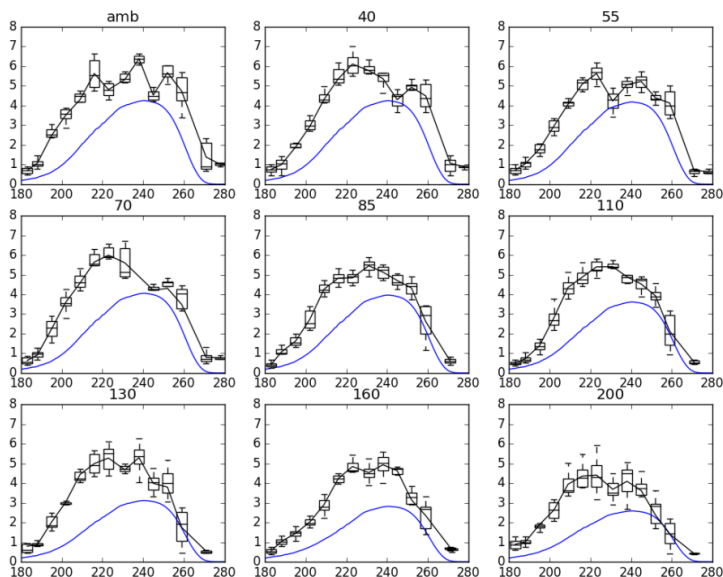
505

Figure 4 Black dashed line is the line of best fit from SoyFACE observation and the blue and green lines with crosses are the modelled output for each ozone concentration using the Osborne et al 2015 tuning with Sitch et al 2007 low and high sensitivity, respectively. The red line and crosses are the tuned parameters with Mead FLUXNET observation and SoyFACE ozone damage according to Table 4 and Figure 8.

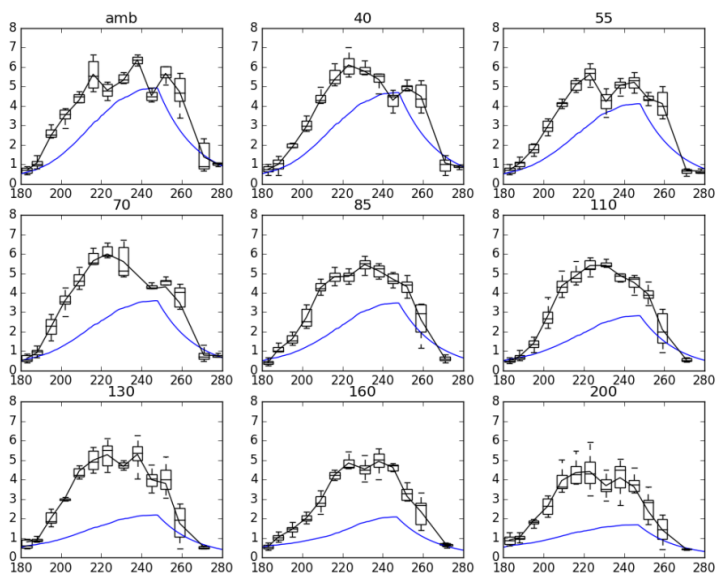
510



LAI (blue: model with mead tuning, black: obs)



LAI (blue: model with osborne2015 tuning, black: obs)



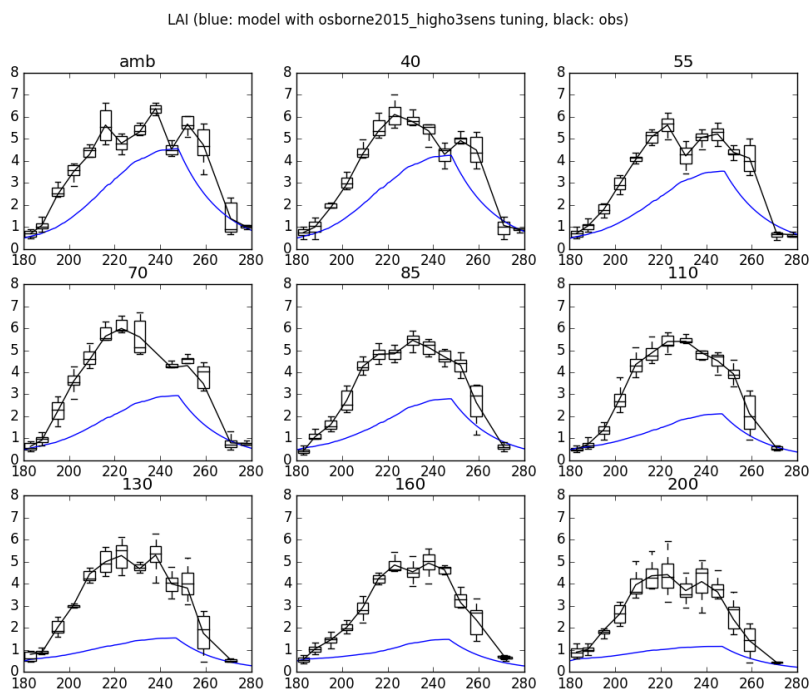


Figure 5 Time series of Leaf Area Index (LAI) responses on different target ozone concentration at SoyFACE.

515 Black line is observed LAI from Betzelberger et al., (2012) and the blue line is JULES-crop LAI. Top:
calibrated JULES-crop using Mead observations. Bottom row: Osborne 2015 tuning with low sensitivity
(middle) and high sensitivity to ozone (bottom).

520

525

530



535

Table 1. JULES modules switches, which F (False) means turned off and T (True) means turned on. Asterisk indicates parameter was hard-wired and the description of the parameters at the bottom

	Osborne et al., (2015)	This study	Discussion
can_rad_mod	5 (6 was not available)	6	Recommended option for layered canopy in version 4.6
l_irrig_dmd	F	T	Irrigation on
irr_crop	-	0	
l_trait_phys	F	F	
l_scale_resp_pm	F	T	
l_leaf_n_resp_fix	F	-	Bug fix, affects can_rad_mod=5 but not can_rad_mod=6
l_prescsow	T	T	Sowing dates available

Parameters	Description
Canopy radiation model	Number 6 is Multi-layer approach for radiation interception following the 2-stream approach of Sellers et al. (1992). This approach takes into account leaf angle distribution, zenith angle, and differentiates absorption of direct and diffuse radiation. it has a decline of leaf N with canopy height. Additionally includes inhibition of leaf respiration in the light. including: Sunfleck penetration though the canopy. Division of sunlit and shaded leaves within each canopy level. A modified version of inhibition of leaf respiration in the light. exponential decline of leaf N with canopy height proportional to LAI, following Beer's law.
L_irrid_dmd	Switch controlling the implementation of irrigation demand code.
Irr_crop	Irrigation season (i.e. season in which crops might be growing on the gridbox) lasts the entire year.
l_trait_phys	Switch for using trait-based physiology. Vcmax is calculated based on parameters nI0 (kgN kgC-1) and neff.
l_scale_resp_pm	Soil moisture stress reduces leaf, root, and stem maintenance respiration.
l_leaf_n_resp_fix	Switch for bug fix for leaf nitrogen content used in the calculation of plant maintenance respiration.
l_prescsow	Sowing dates prescribed

540



545 **Table 2.** Parameter values in JULES-crop that are used to represent soybean. Asterisk indicates parameter was hard-wired.

		Osborne et al., (2015)	This study	Discussion
T_b	Base temperature (K)	278.15	278.15	Kept at Osborne et al., (2015) value
T_o	Optimum temperature(K)	313.15	313.15	Kept at Osborne et al., (2015) value
T_m	Maximum temp (K)	300.15	300.15	Kept at Osborne et al., (2015) value
P_{sen}	Sensitivity of development rate to photoperiod (hours ⁻¹)	0.0	0.0	Kept at Osborne et al., (2015) value
P_{crit}	Critical photoperiod (hours)	-	-	Not used when $P_{sen} = 0$
r_{dir}	coefficient determining relative growth of roots vertically and horizontally	0.0	0.0	Kept at Osborne et al., (2015) value
α_{root}	coefficient of partitioning to root	20.0	19.8	Supplementary Material 1.4.1
α_{stem}	coefficient of partitioning to stem	18.5	18.5	Supplementary Material 1.4.1
α_{leaf}	coefficient of partitioning to leaf	19.5	19.2	Supplementary Material 1.4.1
β_{root}	coefficient of partitioning to root	-16.5	-15.47	Supplementary Material 1.4.1
β_{stem}	coefficient of partitioning to stem	-14.5	-13.195	Supplementary Material 1.4.1
β_{leaf}	coefficient of partitioning to leaf	-15.0	-14.287	Supplementary Material 1.4.1
γ	coefficient of specific leaf area (m ² kg ⁻¹)	25.9	24.0	Supplementary Material 1.4.3
δ	coefficient of specific leaf area (m ² kg ⁻¹)	-0.1451	0.15	Supplementary Material 1.4.3
τ	Remobilisation factor, fraction of stem growth partitioned to RESERVEC	0.18	0.26	Supplementary Material 1.4.3
$fC_{,root}$	Carbon fraction for dry root	0.5	0.47	Supplementary Material 1.4.4
$fC_{,stem}$	Carbon fraction for dry stem	0.5	0.49	Supplementary Material 1.4.4
$fC_{,leaf}$	Carbon fraction for dry leaf	0.5	0.46	Supplementary Material 1.4.4



$f_{C,harv}$	Carbon fraction for harvest	0.5	0.53	Supplementary Material 1.4.4
κ	Allometric coefficient relating STEMC to CANHT	1.6	1.9	Supplementary Material 1.4.2
λ	Allometric coefficient relating STEMC to CANHT	0.4	0.47	Supplementary Material 1.4.2
μ	Allometric coefficient for calculation of senescence	0.05*	5.0	Supplementary Material 1.4.2
ν	Allometric coefficient for calculation of senescence	0.0*	6.0	Supplementary Material 1.4.2
DVI_{sen}	DVI at which leaf senescence begins	1.5*	1.25	Supplementary Material 1.5
C_{init}	Carbon in crop at emergence in kgC/m ² .	0.01*	3.5E-3 (Mead), 7.0E-3 (SoyFACE)	Supplementary Material 1.4.5
DVI_{init}	DVI at which the crop carbon is set to initial carbon	0.0*	0.2	Supplementary Material 1.4.5
T_{mort}	Soil temperature (second level) at t_{bse_io} which to kill crop if $DVI > 1$		263.15	Section 2.3
f_{yield}	Fraction of the harvest carbon pool converted to yield carbon	1.0*	0.74	Section 2.3

550

555

560



Table 3. JULES plant functional type parameters extended to represent soybean. Asterisk indicates parameter was hard-wired.

		Osborne et al., (2015)	This study	Discussion
<i>c3</i>	<i>c3_io</i>	1	1	Soybean is a C3 plant.
<i>dr</i>	<i>rootd_ft_io</i>	0.5	0.5	Not important in irrigated runs, so could not be tuned using US-Ne2 data. Kept at Osborne et al, (2015) value
<i>dqcrit</i>	<i>dq_crit_io</i>	0.1	0.1	Kept at Osborne et al., (2015) value
<i>fa</i>	<i>fd_io</i>	0.015	0.008	Supplementary Material 1.4.6
<i>f0</i>	<i>f0_io</i>	0.9	0.9	Kept at Osborne et al., (2015) value
<i>neff</i>	<i>neff_io</i>	8.0×10^{-4}	12.0×10^{-4}	Table 1
<i>nl(0)</i>	<i>nl0_io</i>	0.073	0.1	Table 1
<i>Tlow</i>	<i>tlow_io</i>	0.0	0.0	Kept at Osborne et al., (2015) value
<i>Tupp</i>	<i>tupp_io</i>	36.0	36.0	Kept at Osborne et al., (2015) value
<i>kn</i>	<i>kn_io</i>	0.78	-	Default for C3 grass for can_rad_mod5.
<i>knl</i>	<i>knl_io</i>	-	0.2	Default for C3 grass for can_rad_mod6.
<i>Q10,leaf</i>	<i>q10_leaf_io</i>	2.0	2.0	Kept at Osborne et al., (2015) value
<i>μrl</i>	<i>nr_nl_io</i>	1.0	0.390	Supplementary Material S1-3
<i>μsl</i>	<i>ns_nl_io</i>	1.0	0.51	Supplementary Material S1-3
<i>rg</i>	<i>r_grow_io</i>	0.25	0.32	Supplementary Material 1.4.6
	<i>orient_io</i>	0	0	Kept at Osborne et al., (2015) value
<i>α</i>	<i>alpha_io</i>	0.12	0.12	Kept at Osborne et al., (2015) value
<i>ωPAR</i>	<i>omega_io</i>	0.15	0.15	Kept at Osborne et al., (2015) value
<i>αPAR</i>	<i>alpar_io</i>	0.1	0.1	Kept at Osborne et al., (2015) value
	<i>fsmc_mod_io</i>	0	0	Not important in irrigated runs, so could not be tuned using US-Ne2 data. Kept at Osborne et al (2015) value.
	<i>fsmc_p0_io</i>	0.0	0.5	FAO document 56 (Allen and Pereira, 2006)
<i>a</i>	<i>can_struct_a_io</i>	1.0	1.0	Kept at Osborne et al., (2015) value



Table 4. Summary of ozone parameter configurations employed in JULES-crop for the default Osborne et al., (2015) value and the tuned as calibrated to SoyFACE leaf gas-exchange measurements (note that these have been calibrated to daytime 8-hour concentrations and therefore will be different to parameters calibrated to monthly 24hour means)

JULES ozone damage Parameters	Fractional reduction of photosynthesis by O ₃ (sensitivity) (mmol m ⁻²) (dfp_dcuo_io)	Threshold of ozone flux (mmol m ⁻² s ⁻¹) (fl_o3_ct_io)
Tuned value	0.5	15.0
Osborne et al 2015 (High sensitivity)	5.0	1.4
Osborne et al 2015 (Low sensitivity)	5.0	0.25

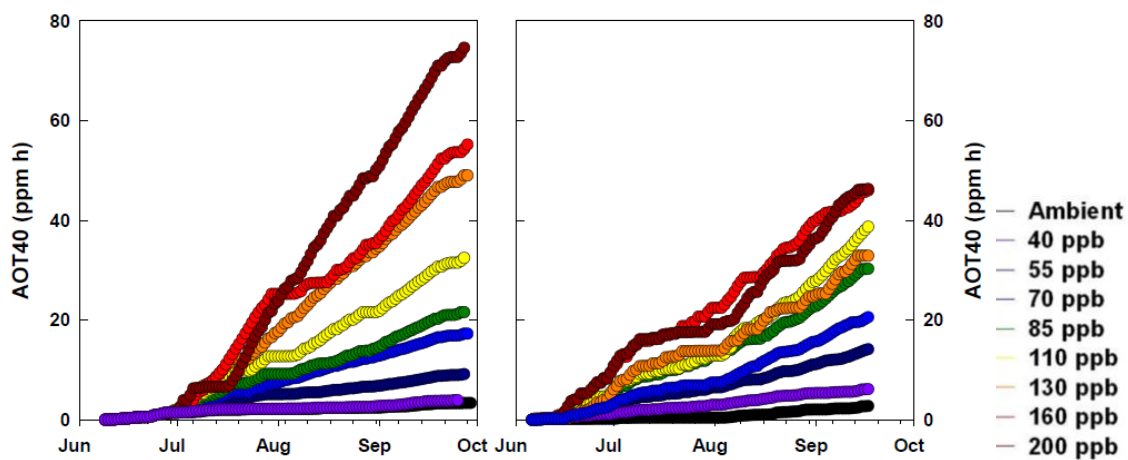


580 **Appendix A**

Table A1 Summary of Land Surface Models (LSM) that contains crop tiles

Crop model	Land Surface Model	Crops Function Type	Scale	Ozone damage on vegetation
LPJ-ml (managed land)	LPJ-GUESS (Bondeau et al., 2007)	13 types of 11 arable crops and 2 managed grass types	Global	No
CLM-CROP	CESM (Community Land Model for Community Earth System Model) (Levis et al., 2011)	Four major crops: maize, soybean, rice and wheat	Global	Yes (Zhang et al., 2018)
Agro-IBIS	IBIS (Kucharik et al., 2003)	12 natural and five crops: Maize, soybean, wheat, <i>Miscanthus giganteus</i> , sugarcane	Continental US	In development
ORCHIDEE-CROP	ORCHIDEE (Gervois et al., 2004; Berg et al., 2010, Wu et al., 2016)	Ten natural and Wheat, maize, soybean, sugarcane and more varieties	Europe and other regions	In development
JULES-Crop	JULES (Clark et al., 2011; Osborne et al., 2015)	4 Crop Functional types, divided into C3 and C4. Potentially 12 crop functional types	Global	Yes. Flux-gradient approach to quantify O ₃ interactive effects.
SIB	Simple Biosphere model (Lokupitiya et al., 2009)	Maize, soybean, wheat	North America	No
ISAM	Integrated Science Assessment Model (Song et al., 2013)	Maize-soybean rotation	North America	No

585



590 **Figure A2** AOT40 measured at SoyFACE in 2009 (left) and 2010 (right). With different target concentration.
(Betzberger et al., 2012)